Estimating the macroscopic capillary length from Beerkan infiltration experiments and its impact on saturated soil hydraulic conductivity predictions

Simone Di Prima, Ryan Stewart, Mirko Castellini, Vincenzo Bagarello, Majdi Abou Najm, Mario Pirastru, Filippo Giadrossich, Massimo Iovino, Rafaël Angulo-Jaramillo, Laurent Lassabatère

Estimating the macroscopic capillary length from Beerkan infiltration experiments

Simone Di Prima [a,b*], Ryan D. Stewart [c], Mirko Castellini [d], Vincenzo Bagarello [e], Majdi R. Abou Najm [f], Mario Pirastru [a], Filippo Giadrossich [a], Massimo Iovino [e], Rafael Angulo-Jaramillo [b] and Laurent Lassabatere [b]

[a] Department of Agricultural Sciences, University of Sassari, Viale Italia, 39, 07100 Sassari, Italy.
[b] Université de Lyon; UMR5023 Ecologie des Hydrosystèmes Naturels et Anthropisés, CNRS, ENTPE, Université Lyon 1, Vaulx-en-Velin, France.
[c] School of Plant and Environmental Sciences, Virginia Polytechnic Institute and State University, Blacksburg, VA, United State.
[d] Council for Agricultural Research and Economics-Agriculture and Environment Research Center (CREA-AA), Via Celso Ulpiani 5, 70125 Bari, Italy.
[e] Department of Agricultural, Food and Forest Sciences, University of Palermo, Palermo, Italy.
[f] Department of Land, Air and Water Resources, University of California, Davis, CA 95616, United States.
* Corresponding Author. E-mail: sdiprima@uniss.it

Abstract

In this investigation, we propose a simple field method for estimating the macroscopic capillary length, λ_c, by only using a single-ring infiltration experiment of the Beerkan type and a measurement of the initial and saturated soil water contents. We assumed that the intercept of the final portion of an experimental infiltration curve could be used as a reliable predictor of the macroscopic capillary length. This hypothesis was validated by assessing the proposed calculation approach using both analytical and field data. The analytical validation demonstrated that the proposed method was able to provide reliable λ_c estimates over a wide range of soil textural characteristics and initial soil water contents. The field testing was performed on a large database including 433 Beerkan infiltration experiments, with the 99.1% of the experiments yielding realistic λ_c values. This method constitutes an easy solution for estimating λ_c, and it can be applied in conjunction with a number λ_c-dependent methods for estimating the saturated soil hydraulic conductivity, K_s, allowing to improve K_s prediction in the field.

Keywords: infiltration, macroscopic capillary length, Beerkan, hydraulic conductivity.

1. Introduction

Gardner (1958) proposed an exponential relation between the soil hydraulic conductivity, K (L T^{-1}) and the water pressure head, h (L):

$$K(h) = K_s exp(\alpha h) \quad (1)$$

where K_s (L T^{-1}) is the saturated soil hydraulic conductivity and α (L^{-1}) is a fitting parameter. Many authors pointed out the importance of the α parameter. For instance, Philip (1985) introduced a parameter related to α called sorptive length that expresses the role of sorption in multidimensional (2-3D) steady state flows. The reciprocal of α, i.e., the macroscopic capillary length, λ_c (L), is a more general length scale parameter that was firstly defined as an integral parameter by Bouwer (1964) (called capillary fringe in his work) and later discussed in detail by White and Sully (1987) and Philip (1985). This parameter expresses the relative importance of gravity and capillary forces during water movement in unsaturated soils (Raats, 1976). More specifically, low λ_c values indicate a dominance of gravity over capillarity, which occurs in coarse-textured and/or highly structured porous media. On the contrary, high λ_c values indicate dominance of capillarity over gravity, which occurs in fine-textured and/or unstructured porous media (Reynolds et al., 2002).

The λ_c parameter depends on the soil hydraulic characteristics and the initial condition (Smith et al., 2002), and is defined as follows (Philip, 1985):

$$\lambda_c = \frac{\phi_m}{\Delta K} \quad (2)$$

where ΔK ($=K_s - K_i$) stands for the difference between K_s and the initial soil hydraulic conductivity, K_i (L T^{-1}), and ϕ_m (L^2T^{-1}) is the matric flux potential, defined by (Gardner, 1958):

$$\phi_m = \int_{h_i}^{0} K(h)dh \qquad h_i \leq h \leq 0 \quad (3)$$

where h_i (L) is the initial soil water pressure head.

Eq. (1) has been used in numerous studies to solve the flow problem (e.g., Philip, 1968; Wooding, 1968). Therefore, the knowledge λ_c has a noticeable practical interest since these parameters were included in many infiltrometer methods for calculating the saturated soil hydraulic conductivity

(Bagarello et al., 2004, 2014d, e.g., 2017; Elrick and Reynolds, 1992; Nimmo et al., 2009; Reynolds and Elrick, 1990; Stewart and Abou Najm, 2018a; Wu et al., 1999). Sometimes, its reciprocal, α, is considered, instead.

Many infiltrometer techniques have been developed overtime to estimate λ_c (e.g., Bagarello et al., 2013; Reynolds and Elrick, 1990; Stewart and Abou Najm, 2018a; Wu et al., 1999). However, all these methods present some limitation. For instance, the two-ponding depths method by Reynolds and Elrick (1990) requires the execution of complicate experiments in the field for measuring the steady state flow rates corresponding to two ponding depths of water. Bagarello et al. (2013) proposed some empirical equations, that however need to be calibrated on experimental infiltration data. Approach 3 by Stewart and Abou Najm (2018b) uses water retention data to constrain λ_c, thus this method requires the estimation of the $\theta(h)$ relationship. Other methods are based on the analysis of transient state data, as for the case of the method 1 by Wu et al. (1999) and Approach 2 by Stewart and Abou Najm (2018a), that need an accurate and often not easy to obtain description of the transient state (Di Prima et al., 2019). Therefore, alternative methods for estimating λ_c from simple and easily replicable infiltration experiments could substantially reduce the amount of work necessary to obtain accurate estimates of soil hydraulic properties in the field (Bagarello et al., 2014d).

The objective of this investigation was to validate a simple field method to estimate the macroscopic capillary length by only using a single-ring infiltration experiment of the Beerkan type (Lassabatere et al., 2006) and a measurement of the initial and saturated soil water contents. The theoretical analysis was initially developed. The proposed method was then validated using analytically generated data and a Beerkan infiltration database including 433 field experiments.

2. Theory

According to White and Sully (1987), Eq. (2) could be rewritten as:

$$\lambda_c = \frac{b\,S^2}{(\Delta\theta\,\Delta K)} \quad (4)$$

where b is a dimensionless constant dependent on the shape of the soil water diffusivity function, S (L $T^{-0.5}$) is the soil sorptivity (Philip, 1957), $\Delta\theta$ ($=\theta_s - \theta_i$) stands for the difference between the saturated, θ_s (L^3L^{-3}), and initial, θ_i (L^3L^{-3}), volumetric soil water content. For field soils, b is commonly set equal to 0.55 and K_i is negligible (White and Sully, 1992).

The estimation of the macroscopic capillary length with equation (4) requires the previous determination of sorptivity and hydraulic conductivity. These quantities can be estimated thanks to water infiltration experiments and fitting to the quasi-exact implicit (QEI) model developed by Haverkamp et al. (1994) or its related approximate expansions (see Lassabatere et al., 2009 for more details). Haverkamp et al. (1994) proposed the following approximate expansion for the description of the steady-state for water infiltrated through a disc source while maintaining a zero water pressure head at surface:

$$I_{3D}^{+\infty}(t) = \left(K_s + \frac{\gamma S^2}{r\Delta\theta}\right) t + \frac{S^2}{2(1-\beta)\Delta K} ln\left(\frac{1}{\beta}\right) \quad (5)$$

Where r (L) is the radius of the source, γ and β are two infiltration constants, often fixed at 0.75 and 0.6, respectively (Haverkamp et al., 1994). b_s (L) and i_s (L T^{-1}) that are the intercept and slope of the steady state approximate expansion are defined as a function of hydraulic conductivity and sorptivity as follows:

$$i_s = K_s + \frac{\gamma S^2}{r_d\Delta\theta} \quad (6a)$$

$$b_s = \frac{S^2}{2(1-\beta)\Delta K} ln\left(\frac{1}{\beta}\right) \quad (6b)$$

In this study, we use the equation defining the intercept, b_s, to quantify the ratio between sorptivity and the difference in hydraulic conductivity, as already suggested by Castellini et al. (2018):

$$\frac{S^2}{\Delta K} = \frac{b_s}{C} \quad (7a)$$

$$C = \frac{1}{2(1-\beta)} ln\left(\frac{1}{\beta}\right) \quad (7b)$$

The implementation of such expression into equation (4) leads to the following expression for the macroscopic capillary length:

$$\lambda_c = \frac{b}{\Delta\theta}\frac{b_s}{C} \quad (8)$$

Eq. (8) constitutes a considerable simplification, allowing to estimate the macroscopic capillary length, λ_c, by only using the infiltration experiment and a measurement of difference between the initial and saturated soil water contents, $\Delta\theta$. Indeed, once the intercept of the steady state, b_s, is estimated, using for instance the linear regression of the last points of the cumulative infiltration, and once the parameter b is determined, λ_c can be easily determined. Note that White and Sully (1987) fixed b at 0.55 for the case when the initial hydraulic conductivity is far lower than the saturated hydraulic conductivity, $K_i \ll K_s$. In addition, β is fixed at 0.6, leading to a value of 0.639.

The previous estimation of the macroscopic capillary length may allow the estimation of the saturated hydraulic conductivity. Many methods for calculating the saturated soil hydraulic conductivity from single-ring data require an estimation of λ_c or its inverse α. Thus, in this investigation, we also assessed the impact of the proposed approach on K_s calculation. Among the λ_c-dependent methods, we considered the following methods for estimating the saturated hydraulic conductivity:

i) the One-Ponding Depth (**OPD**) method by Reynolds and Elrick (1990);

ii) the method 2 by Wu et al. (1999) (**WU2**);

iii) the Steady version of the Simplified method based on a Beerkan Infiltration run (**SSBI**) by Bagarello et al. (2017);

iv) the Approach 4 (**A4**) by Stewart and Abou Najm (2018b).

All these calculation procedures have been detailed in **Table E**. For this investigation, only steady state methods have been selected because the proposed λ_c estimation procedure is also based on steady state data analysis, thus they all consider the same experimental information. In addition, the late phase of the infiltration process is easier to interpret in comparison to the transient state (Di Prima et al., 2018a), which is frequently subjected to different and sometimes simultaneous perturbations, especially on water repellent soils or soils with macropores (Angulo-Jaramillo et al., 2019).

3. Material and methods

3.1. Analytically generated data

We assessed the accuracy of the proposed calculation approach to yield reliable λ_c and K_s predictions by using the same six soils (i.e., sand, loamy sand, sandy loam, loam, silt loam, silty clay loam) considered by Hinnell et al. (2009) and Bagarello et al. (2017) to cover a wide range of hydraulic responses. We modelled the infiltration experiments for these synthetic soils using the parameters listed by Carsel and Parrish (1988) to describe the water retention curve and the hydraulic conductivity function according to the van Genuchten–Mualem model (Mualem, 1976; van Genuchten, 1980) (**Table C**):

$$\begin{cases} \theta(h) = \theta_r + (\theta_s - \theta_r)[1 + \alpha_{VG}|h|^n]^{-m} & h < 0 \\ \theta(h) = \theta_s & h \geq 0 \end{cases} \quad (9a)$$

$$m = 1 - \frac{1}{n} \quad (9b)$$

$$K(h) = \widehat{K}_s Se^l \left[1 - \left(1 - Se^{1/m}\right)^m\right]^2 \quad (9c)$$

where $\widehat{K}_s$ (L T^{-1}) is the actual value of the saturated soil hydraulic conductivity, α_{VG} is an empirical parameter related to the inverse of the air-entry pressure head, n is the pore size distribution index, $Se = (\theta - \theta_r)/(\theta_s - \theta_r)$ is the effective saturation degree, θ_r (L^{3}L^{-3}) is the residual water content, l is the pore connectivity parameter, assumed to be 0.5 by Mualem (1976). To also test the effect of the initial soil water content on parameters predictions, initial values of Se ranging from 0.1 to 0.8 were considered when modeling infiltration. For a given soil and an initial Se value, the actual value of the macroscopic capillary length, $\hat{\lambda}_c$, was estimated by Eq. (2).

The cumulative infiltration curves were generated using the infiltration model proposed by Haverkamp et al. (1994). More specifically, for any zero or negative value of the pressure head at the soil surface, 1D cumulative infiltration, I_{1D} (L), into an initially uniform unsaturated soil profile can be modelled by the following 1D implicit equation (Haverkamp et al., 1990):

$$\frac{2\Delta K^2}{S^2}t = \frac{1}{1-\beta}\left[\frac{2\Delta K}{S^2}(I_{1D}(t) - K_i t) - ln\left(\frac{exp\left(2\beta\frac{\Delta K}{S^2}(I_{1D}(t)-K_i t)\right)+\beta-1}{\beta}\right)\right] \quad (10)$$

with $\Delta K = \widehat{K}_s - K_i$. Eq. (10) was extended to three-dimensional (3D) infiltration from a surface disk source by Smettem et al. (1994), adding a term representing 3D geometrical effects [see Eq. (23) of Smettem et al., 1994]:

$$I(t) = I_{1D}(t) + \frac{\gamma S^2}{r_d \Delta\theta} \quad (11)$$

where I is 3D cumulative infiltration, γ is a shape parameter for geometrical correction of the infiltration front shape, commonly set at 0.75 for $\theta_i < 0.25\ \theta_s$ (Haverkamp et al., 1994). For a given soil and an initial Se value, sorptivity was estimated from soil hydraulic properties in the interval of soil water pressure head between h_i and 0 as follows (Parlange, 1975):

$$S = \sqrt{\int_{h_i}^{0}(\theta_s + \theta - 2\theta_i)K(h)dh} \quad (12)$$

Then, Eqs. (10) and (11) were used to generate cumulative infiltration curves. Shape parameters β and γ were assumed equal to the default values, i.e., 0.6 and 0.75, respectively (Angulo-Jaramillo et al., 2019). The duration of the infiltration process was fixed at three times the maximum time, t_{max} (T), for which the transient expression of the 3D Haverkamp equation (see Eq. (3a) in Lassabatere et al. 2006) can be considered valid, with t_{max} calculated as follows (Lassabatere et al., 2006):

$$t_{max} = \frac{1}{4(1-B)^2}\left(\frac{S}{\widehat{K}_s}\right)^2 \quad (13a)$$

$$B = \frac{2-\beta}{3}\left(1 - \frac{K_i}{\widehat{K}_s}\right) + \frac{K_i}{\widehat{K}_s} \quad (13b)$$

These analytical data were used to estimate the intercept, b_s, and the slope, i_s, by linear regression analysis of the last three data points of the cumulative infiltration versus time plot, which were assumed to provide a reliable description of steady state conditions. Then, we estimated λ_c and K_s by Eqs. (8) and (t1-4), respectively. These estimates were compared with the corresponding actual values, i.e., the $\hat{\lambda}_c$ values estimated with Eq. (2) and the $\hat{K}_s$ values by Carsel and Parrish (1988) listed in **Table C**, using the relative error, *Er*, defined as follows:

$$Er(x) = 100 \times \frac{x-\hat{x}}{\hat{x}} \quad (14)$$

Where $\hat{x}$ is the actual value for $\hat{\lambda}_c$ or $\hat{K}_s$ and x is the corresponding estimated value λ_c or K_s. Note that positive $Er(x)$ values indicate overestimations whereas negative values indicate underestimations. Small deviations, i.e., $Er(x) \sim 0$, suggest that the estimated soil hydraulic parameters are close to actual values. According to the accuracy criterion by Reynolds (2013), the estimates were deemed accurate when they fell within the range $0.75 \leq x/\hat{x} \leq 1.25$ (i.e. ≤ 25% error). Such a stringent accuracy criterion was used because the parameters were estimated by analytically generated data, and therefore they were free of the perturbations embedded in field and laboratory measurements (e.g., measurement error, random noise and natural variability).

3.2. The Beerkan infiltration database

In this investigation we considered a large database of Beerkan infiltration experiments carried out in four different countries, i.e., Italy, Burundi, France and Spain, during the period 2010-2017 (**Table S**). However, nearly half of the runs, i.e., the 46.7% were carried out in Sicily (Italy) (202 out of 433). While, the 35,1% of the runs (152 out of 433) were carried out in Burundi in the African great lakes region. The runs were carried out at 433 sampling points on soils having contrasting textural characteristics, i.e., from sandy to clayey (**Figure T**).

All Beerkan experiments were carried out according to the methodology described by Lassabatere et al. (2006). As prescribed by the Beerkan method, a stainless steel ring was inserted shallowly into the soil (~1 cm). For each run, different volumes of water were successively poured on the confined soil surface. The number of poured volumes varied depending on time needed to reach steady state, as required by the Beerkan method (Angulo-Jaramillo et al., 2019). The Beerkan experiments considered in this investigation were performed using rings with inner diameters from 5 to 30 cm. The volume of water for each pouring was chosen in order to establish ponding condition on the entire infiltration surface; the volumes ranged from 17 to 800 mL, depending on the used ring (**Table S**). The energy of the falling water was dissipated with fingers to minimize the soil disturbance owing to water pouring, as commonly suggested (e.g., Di Prima et al., 2019). For each poured volume, the time needed for the water to infiltrate was recorded, and the cumulative infiltration, I (mm), was plotted against time, t (h).

Similarly to the procedure previously described to analyse analytical generated curves, for each Beerkan experiment we estimated the intercept, b_s (mm), and the slope, i_s (mm h^{-1}), of the regression line fitted to the data points describing steady state conditions. Then, we estimated λ_c and K_s by Eqs. (8) and (t1-4), respectively.

For the field data, we chose not to use a reference λ_c value, as an independent datum that can be used for assessing simplified procedures or validating new developed methods does not currently exist. In addition, methods for estimating λ_c from single-ring infiltration experiments are based on cumbersome field procedures.

According to Elrick and Reynolds (1992), we classified the λ_c estimates in five soil capillarity categories, i.e., from negligible ($\lambda_c \leq 10$ mm) to very strong ($\lambda_c \geq 1000$ mm) (**Table L**). Note that these categories were originally proposed to select a representative value of the sorptive number, α (L^{-1}), which is equal to λ^{-1}, on the basis of five soil texture-structure categories when calculating K_s by the OPD method (Angulo-Jaramillo et al., 2016). In this investigation, we also propose range values for each category as detailed in **Table L**.

For K_s, we used as a benchmark the values obtained with the BEST-steady method proposed by Bagarello et al. (2014c), which estimates K_s as follows:

$$K_{s,BEST} = \frac{C\, i_s}{A\, b_s + C} \qquad (15a)$$

$$A = \frac{\gamma}{r(\theta_s - \theta_i)} \qquad (15b)$$

Thus, the K_s values estimated by Eqs. (t1-4) were compared with those obtained by Eq. (15) in terms of relative errors using Eq. (14). We chose this method, as it involves the same experimental information of the λ_c-dependent methods considered in this investigation for estimating K_s, but it does not require an estimation of λ_c.

We avoided to use laboratory measurements as benchmark, as they can induce experimental artifacts (Haverkamp et al., 1999), such as soil compaction and samples biased by pores, that may limit their comparability with in-situ measurements (e.g., Bagarello et al., 2009; Di Prima et al., 2018c). Discrepancies are also expected when different measurement techniques are applied in the field or even when the same dataset is analyzed by alternative calculation approaches (Mertens et al., 2002), though in the latter case the results can still be compared to one another (Wu et al., 1999).

For comparisons between paired observations, the paired differences, i.e., $K_s - K_{s,BEST}$ for given method, were calculated and the hypothesis of normality of these differences was checked by the Kolmogorov-Smirnov test. For non-normally distributed data the Wilcoxon signed rank test was used to test the median difference between paired observations at $P < 0.05$.

4. Results

4.1. Analytical validation

4.1.1. Actual values of the macroscopic capillary length

As expected, Eq. (2) yielded higher $\hat{\lambda}_c$ values for fine-textured soils and lower Se values (**Table P**). This is logical, since for fine soils the capillary contribution to water flow was higher than for coarser soils. More specifically, high λ_c values are associated to initially flat $K(h)$ relationships, i.e., when a decrease in pressure head determines a moderate pore emptying (Angulo-Jaramillo et al., 2016; Reynolds, 1994). As an example, this behavior can be observed on the hydraulic conductivity function of the silty clay loam soil (**Figure K)**, where the functional relationship between K and Se is very flat for low Se values, i.e. high pressure head. On the other hand, low λ_c values are associated to steep relationships, i.e., when a small decrease in pressure head determines a more relevant pore emptying (e.g., sand, **Figure K**).

4.1.2. Estimating λ_c from analytically generated data

Cumulative infiltration could be calculated for all cases trough Eqs. (10) and (11) and using the parameters listed in **Table C**. All curves exhibited usual shapes, with a concave shape as a function of time, due to a decreasing hydraulic gradient as the wetting front moves away from the source and the influence of capillarity decreases (Xu et al., 2012). As the process approaches steady state, cumulative infiltration curves become approximately linear with time (Angulo-Jaramillo et al., 2016) (**Figure H**). Note that the duration of the infiltration process decreased for higher values of the initial effective saturation degree. Indeed, for wetter initial conditions steady state was reached more quickly and with less water (Di Prima et al., 2016). In this case, the influence of capillary forces on infiltration was very short, and the cumulative infiltration curves exhibited a more linear shape (Angulo-Jaramillo et al., 2019).

The values of the intercept, b_s, estimated from these curves, were used in conjunction with the θ_i and θ_s values to calculate λ_c by Eq. (8) (**Table P**). Then, the λ_c values were compared with the corresponding actual values, $\hat{\lambda}_c$, in terms of relative errors (**Figure G**). All λ_c values were accurate according to the chosen criterion, since $Er(\lambda_c)$ ranged from -23.2 to 7.9%. The higher $|Er(\lambda_c)|$ values were obtained for the coarse-textured soils, namely the sandy and loamy sand soils, and only for initial wet conditions (**Figure G**). Under these conditions, the ratio K_i / K_s departed from the assumption made to approximate Eq. (7a) (i.e., $K_i \ll K_s$). More specifically, near the saturation, the ratio K_i / K_s was higher for the coarser soils than for the fine-textured soils because the capillary forces were weaker and the increase of the hydraulic conductivity near the saturation was less abrupt (**Figure K**). As a consequence, for the coarser soils, neglecting the K_i / K_s ratio in Eq. (7a) negatively affected λ_c estimates, yielding higher errors. Nevertheless, λ_c estimates were sufficiently accurate also in these cases, with errors always lower than 25%.

4.1.3. Estimating K_s from analytically generated data

The values of the slope, i_s, estimated from the analytically generated curve, were used to calculate K_s by the four λ_c-dependent methods (i.e., OPD, WU2, SSBI, A4) using Eqs. (t1-4) (**Table P**). Then, the K_s values were compared with the corresponding actual values, $\widehat{K}_s$ (**Table C**), in terms of relative errors (**Figure W**). The $Er(K_s)$ values ranged from -3.1 to 9.5%, from -7.4 to 5.4%, from -24.7 to -2.2%, and from 2.4 to 14%, for the OPD, WU2, SSBI and A4 methods, respectively. Mean $|Er(K_s)|$ values were ordered as OPD < A4 < WU2 < SSBI. Therefore, the OPD method was the most accurate overall. However, the four methods always yielded accurate estimates, since $|Er(K_s)|$ values were always lower than 25% (**Figure W**).

4.2. Field testing

4.2.1. Peculiarities and experiments exclusion

For six Beerkan experiments infiltration rates increased with time, such that the cumulative infiltration curves exhibited convex shapes. The cumulative infiltration data in that instance yielded a negative value for the intercept, b_s. This circumstance led to negative λ_c data. In addition, in case of negative intercept values, the BEST-steady algorithm is also expected to estimate meaningless K_s data (Angulo-Jaramillo et al., 2019). For this reason these Beerkan experiments were excluded from subsequent analyses. These cases occurred at the Kinyami site (two instances), Palermo - SAAF site (one instance) and Crépieux-Charmy site (three instances), and reflect that the early wetting phase was impeded due to soil water repellency (Concialdi et al., 2019). Hydrophobia may be attributed to locally high OC content (Goebel et al., 2011), exudates produced by the plant root systems or living organisms like arbuscular mycorrhizal fungi (Rillig et al., 2010), and organic pollutants such as hydrocarbons (Durand et al., 2005).

4.2.2. Estimating λ_c from the Beerkan infiltration database

The Beerkan experiments that were not affected by flow impedance (427 out of 433) could be analyzed to determine λ_c. Eq. (8) yielded λ_c values ranging from 1.5 to 737.7 mm (**Table Q**).

According to the soil capillarity categories suggested by Elrick and Reynolds (1992), the λ_c values were classified as representative of strong capillarity conditions in 29.7% of the cases (127 out of 427), moderate in the 44.3% (189), weak in the 25.1% (107), and negligible in the 0.9% (4) (**Figure D**). The categories weak and negligible were associated with the higher sand contents, i.e., 35% and 37%, respectively. Thus, for the field experiments, Eq. (3) estimated the lowest λ_c values for the coarsest soils, i.e., when gravity was expected to prevail over capillarity. This result increases our confidence on the proposed calculation approach.

Three different examples of λ_c estimation are shown in **Figure Fb-d**. The cases differs by the regime of the infiltration process and the shape of the cumulative infiltration. More specifically, we considered: i) an infiltration process that is initially capillary driven and then, at the late phase, both capillary and gravity driven (first case, **Figure Fb**), ii) an infiltration processes dominated by capillarity (second case, **Figure Fc**), and an infiltration processes dominated by gravity (third case, **Figure Fd**). According to Angulo-Jaramillo et al. (2019), these cases correspond to three typical responses when applying the Beerkan protocol respectively on i) regular soils, ii) very fine soils and iii) very coarse soils (see their Figure 13).

In the first case (**Figure Fb**), cumulative infiltration exhibits an usual concave shape as a function of time. For this run, we estimated an intercept value of 30.9 mm, and a λ_c value of 49.2 mm falling within the range of $42 \leq \lambda_c \leq 125$ mm (**Figure Fa**). According to the capillarity categories suggested by Elrick and Reynolds (1992), the estimated λ_c value is representative of moderate capillarity conditions (**Table L**).

In the second case (**Figure Fc**), the cumulative infiltration curve exhibits a strong concave shape with an intercept value of 209.6 mm, yielding a λ_c value of 598.7 mm, falling within the strong capillary category (**Table L** and **Figure Fa**). This behavior is typical for very fine soils, with low permeability. For this run, capillary forces predominates for almost the duration of the experiment and the attainment of steady state required more time (Di Prima et al., 2016).

In the third case (**Figure Fd**), the cumulative infiltration curve exhibits an almost linear shape with an intercept value of 1.0 mm, yielding a λ_c value of 1.5 mm, i.e., lower than the considered threshold of 10 mm for negligible capillarity forces (**Table L** and **Figure Fa**). This behaviour is typical for coarse-textured soils and occurs when the infiltration process is mainly driven by gravity. Negligible values of λ_c were also reported in other investigations (e.g., Khaleel and Relyea, 2001; Russo et al., 1997; White and Sully, 1992). In this investigation we obtained negligible λ_c values in only four cases out of 427. These cases corresponded to the lowest measured intercept values (**Figure Fa**).

4.2.3. Estimating K_s from the Beerkan infiltration database

The differences between K_s and $K_{s,BEST}$ were always non-normally distributed according to the Kolmogorov-Smirnov test. The Wilcoxon signed rank test showed that the four methods (i.e., OPD, WU2, SSBI, A4) yielded K_s estimates significantly different from the BEST-steady values. However, the discrepancies between methods were always lower than ≤ 25%, with the exception of the SSBI method (**Figure Z**). More specifically, the method that yielded the lowest discrepancies was the WU2 method. This method yielded K_s values ranging from 1.4 to 3493.8 mm h^{-1} (**Table Q**), with 76 and 24% of the runs yielding respectively lower and higher K_s estimates than the BEST-estimated values (**Figure Z**). The median K_s values differed by only a factor of 1.002. The relative error, $Er(K_s)$, ranged from -12.1 to 22.1%. Therefore, according to selected criterion (i.e., discrepancies ≤ 25%), the WU2 and BEST-steady methods yielded similar K_s estimates. The OPD and A4 methods also gave $|Er(K_s)|$ values always lower than 25%, suggesting that also these methods yielded similar K_s estimates to those values obtained by BEST-steady. Larger discrepancies were only obtained when using the SSBI method. This method always yielded K_s values higher than $K_{s,BEST}$, with only one exception. The $Er(K_s)$ values ranged from -1.0 to 32.8%, with 21% of the runs (88 out of 427) yielding higher values than the considered threshold of 25%.

5. Discussion

In this investigation, we proposed to estimate the macroscopic capillary length using a simple Beerkan infiltration experiment and a measurement of the initial and saturated soil water contents. Previous investigations also suggested that the measured infiltration curve contains the necessary information to estimate λ_c (Bagarello et al., 2013, e.g., 2014d; Stewart and Abou Najm, 2018a; Wu et al., 1999). However, these methods are based on the analysis of the transient infiltration process. Indeed, they all require an estimation of the infiltration coefficients by the fitting of transient models to early infiltration data. It is not uncommon that these methods perform poorly, especially in case of uncertainties on the transient phase (e.g., Di Prima et al., 2019, 2018b). While these methods may alleviate the experimental efforts needed to determine λ_c and K_s in the field, for instance, reducing the required measurement time for low permeability soils (Bagarello et al., 2014d), they may introduce uncertainties on the hydraulic characterization and increase parameter variability (Di Prima et al., 2018b). This limitation can ultimately complicate an accurate assessment of spatial-temporal variability of soil hydraulic properties (Angulo-Jaramillo et al., 2016).

On the other hand, the proposed method uses the experimental information collected during the final stage of the infiltration process, thus, it is expected to be less sensitive to experimental data accuracy (Bagarello et al., 2013). Estimating λ_c requires the intercept (b_s) that can be easily calculated by linear regression analysis of the final portion of the cumulative infiltration. While the final infiltration rate (i_s) is totally independent from the early phase of the infiltration process, the intercept depends on the shape of the cumulative infiltration curve, thus, it restitutes a certain information on the transient phase (Bagarello et al., 2014c). The shape of the cumulative infiltration, in turn, reveals the relative importance of capillary and gravity forces during a ponding infiltration process, being more concave or linear respectively in case of prevalence of capillarity over gravity or vice versa (Angulo-Jaramillo et al., 2019). More specifically, small values of the intercept are indicative of a linear infiltration curve, i.e., when gravity prevails over capillarity, which occurs primarily in coarse-textured and/or highly structured porous media. On the contrary, high intercept values are indicative of a concave infiltration curve, i.e., when capillarity prevails over gravity, which occurs primarily in fine-textured soils. Therefore, b_s is expected to be a reliable predictor of the macroscopic capillary length.

In this investigation, this hypothesis was validated by assessing the proposed calculation approach using both analytical and field data. The analytical validation demonstrated that Eq. (8) was able to provide reliable λ_c estimates over a wide range of soil textural characteristics and initial soil water contents. We also tested the new method on a large database including 433 Beerkan infiltration experiments carried out on different soils having contrasting textural characteristics, i.e., from sandy to clayey. The 99.1% of the experiments yielded λ_c values falling within the realistic range $10 \leq \lambda_c \leq 1000$ mm (W. D. Reynolds and Elrick, 2002), with the only expectation of four cases yielding negligible λ_c values, i.e., lower than 10 mm.

An expected advantage of the proposed method is to improve K_s prediction since it avoids to choose a λ_c value on the basis of the soil capillarity categories. Indeed, using Eqs. (t1-4) needs knowledge of λ_c, that, according to Elrick and Reynolds (1992), can be estimated on the basis of a general description of soil textural and structural characteristics (**Table L**). The effect of an erroneous choice of the capillarity category on K_s predictions was investigated by Bagarello et al. (2014d). These authors assessed the sensitivity of K_s to the right choice of the capillarity category, reporting that an erroneous choice of the capillarity category, for instance differing by plus or minus one category from the correct one, may also lead to discrepancies between K_s estimates of more than a factor of three. A sensitivity analysis to determine the effect of errors in constraining λ_c on K_s estimations was also performed by Stewart and Abou Najm (2018b). These authors reported that K_s estimates are more sensitive to underpredictions of λ_c compared with overpredictions. Therefore, choosing an erroneous λ_c value from the previous capillarity category may have a more relevant effect than choosing the λ_c value from the successive category. In any case, the subjectivity on the choice of an appropriate λ_c value constitutes a clear limitation when using λ_c-dependent methods for estimating K_s, such as those considered in this investigation. On the contrary, the proposed method avoids any subjectivity on the estimation of λ_c.

A possible limitation when using this calculation approach, especially on very fine soils, is related to the need of infiltrating enough water during the experiment in order to approach steady state conditions. Indeed, fine-textured and unstructured soils often exhibit very low permeability, thus, the attainment of steady state may require excessively long experiments (Di Prima et al., 2016), which would complicate reaching steady state conditions with the regular Beerkan protocol (Alagna et al., 2016a). This problem can be easily solved using automated devises, such as the one developed by Di Prima (2015) and Concialdi et al. (2019), that allows accurate and automated infiltration rates measurements. The first obvious advantage in using automatic infiltrometer in case of low permeability soils is that data collection is automated and it does not require any further manipulation by the user once the device is installed. Therefore, tests can be simultaneously performed alleviating the experimental efforts in case of long experiments durations (Alagna et al., 2018).

6. Summary and conclusions

In this investigation, we assessed a simple field method for estimating the macroscopic capillary length, λ_c, by only using a single-ring infiltration experiment of the Beerkan type and a measurement of the initial and saturated soil water contents. We validated the proposed method by using both analytical generated data and a large database of 433 Beerkan infiltration experiments carried out in four different countries, i.e., Italy, Burundi, France and Spain, during the period 2010-2017. While the analytical validation supported our hypothesis that the intercept, b_s, is a reliable predictor of the macroscopic capillary length, the testing carried out using the Beerkan database increased our confidence on the proposed calculation approach. This method constitutes an easy solution to estimate λ_c, and it can be applied in conjunction with a number of λ_c-dependent methods for estimating the saturated soil hydraulic conductivity, allowing to improve K_s prediction in the field. The proposed method may also avoid any subjectivity caused by the selection of a representative λ_c value on the only base of textural and structural characteristics.

Funding: This work was supported through the INFILTRON Project (ANR-17-CE04-0010, Package for assessing infiltration & filtration functions of urban soils in stormwater management; https://infiltron.org/) funded by the French National Research Agency (ANR), and the "Programma Operativo Nazionale (PON) Ricerca e Innovazione 2014-2020 (Linea 1 - Mobilità dei ricercatori, AIM1853149, CUP: J54I18000120001) funded by the European Regional Development Fund (ERDF) and the Italian Ministry of Education, University and Research (MIUR).

Author Contributions: S. Di Prima outlined the investigation, developed the theory and analyzed the data. All authors contributed to discussing the results and writing the manuscript.

Conflicts of Interest: The authors declare no conflict of interest.

References

Alagna, V., Bagarello, V., Di Prima, S., Giordano, G., Iovino, M., 2016a. Testing infiltration run effects on the estimated water transmission properties of a sandy-loam soil. Geoderma 267, 24–33. https://doi.org/10.1016/j.geoderma.2015.12.029

Alagna, V., Bagarello, V., Di Prima, S., Iovino, M., 2016b. Determining hydraulic properties of a loam soil by alternative infiltrometer techniques. Hydrological Processes 30, 263–275. https://doi.org/10.1002/hyp.10607

Alagna, V., Iovino, M., Bagarello, V., Mataix-Solera, J., Lichner, Ľ., 2018. Alternative analysis of transient infiltration experiment to estimate soil water repellency. Hydrological Processes. https://doi.org/10.1002/hyp.13352

Angulo-Jaramillo, R., Bagarello, V., Di Prima, S., Gosset, A., Iovino, M., Lassabatere, L., 2019. Beerkan Estimation of Soil Transfer parameters (BEST) across soils and scales. Journal of Hydrology 576, 239–261. https://doi.org/10.1016/j.jhydrol.2019.06.007

Angulo-Jaramillo, R., Bagarello, V., Iovino, M., Lassabatère, L., 2016. Infiltration Measurements for Soil Hydraulic Characterization. Springer International Publishing.

Bagarello, V., Castellini, M., Di Prima, S., Giordano, G., Iovino, M., 2013. Testing a Simplified Approach to Determine Field Saturated Soil Hydraulic Conductivity. Procedia Environmental Sciences 19, 599–608. https://doi.org/10.1016/j.proenv.2013.06.068

Bagarello, V., Castellini, M., Di Prima, S., Iovino, M., 2014a. Soil hydraulic properties determined by infiltration experiments and different heights of water pouring. Geoderma 213, 492–501. https://doi.org/10.1016/j.geoderma.2013.08.032

Bagarello, V., Di Prima, S., Giordano, G., Iovino, M., 2014b. A test of the Beerkan Estimation of Soil Transfer parameters (BEST) procedure. Geoderma 221–222, 20–27. https://doi.org/10.1016/j.geoderma.2014.01.017

Bagarello, V., Di Prima, S., Iovino, M., 2017. Estimating saturated soil hydraulic conductivity by the near steady-state phase of a Beerkan infiltration test. Geoderma 303, 70–77. https://doi.org/10.1016/j.geoderma.2017.04.030

Bagarello, V., Di Prima, S., Iovino, M., 2014c. Comparing Alternative Algorithms to Analyze the Beerkan Infiltration Experiment. Soil Science Society of America Journal 78, 724. https://doi.org/10.2136/sssaj2013.06.0231

Bagarello, V., Di Prima, S., Iovino, M., Provenzano, G., 2014d. Estimating field-saturated soil hydraulic conductivity by a simplified Beerkan infiltration experiment. Hydrological Processes 28, 1095–1103. https://doi.org/10.1002/hyp.9649

Bagarello, V., Di Prima, S., Iovino, M., Provenzano, G., Sgroi, A., 2011. Testing different approaches to characterize Burundian soils by the BEST procedure. Geoderma 162, 141–150. https://doi.org/10.1016/j.geoderma.2011.01.014

Bagarello, V., Iovino, M., Elrick, D., 2004. A Simplified Falling-Head Technique for Rapid Determination of Field-Saturated Hydraulic Conductivity. Soil Science Society of America Journal 68, 66. https://doi.org/10.2136/sssaj2004.6600

Bagarello, V., Sferlazza, S., Sgroi, A., 2009. Testing laboratory methods to determine the anisotropy of saturated hydraulic conductivity in a sandy–loam soil. Geoderma 154, 52–58. https://doi.org/10.1016/j.geoderma.2009.09.012

Bouwer, H., 1964. Unsaturated Flow in Ground-Water Hydraulics. Journal of the Hydraulics Division 90, 121–144.

Carsel, R.F., Parrish, R.S., 1988. Developing joint probability distributions of soil water retention characteristics. Water Resour. Res. 24, 755–769. https://doi.org/10.1029/WR024i005p00755

Concialdi, P., Di Prima, S., Bhanderi, H.M., Stewart, R.D., Abou Najm, M.R., Gaur, M.L., Angulo-Jaramillo, R., Lassabatere, L., 2019. An open-source instrumentation package for intensive soil hydraulic characterization. Submitted to Journal of Hydrology.

Di Prima, S., 2015. Automated single ring infiltrometer with a low-cost microcontroller circuit. Computers and Electronics in Agriculture 118, 390–395. https://doi.org/10.1016/j.compag.2015.09.022

Di Prima, S., Bagarello, V., Lassabatere, L., Angulo-Jaramillo, R., Bautista, I., Burguet, M., Cerdà, A., Iovino, M., Prosdocimi, M., 2017. Comparing Beerkan infiltration tests with rainfall simulation experiments for hydraulic characterization of a sandy-loam soil. Hydrological Processes 31, 3520–3532. https://doi.org/10.1002/hyp.11273

Di Prima, S., Castellini, M., Abou Najm, M.R., Stewart, R.D., Angulo-Jaramillo, R., Winiarski, T., Lassabatere, L., 2019. Experimental assessment of a new comprehensive model for single ring infiltration data. Journal of Hydrology 573, 937–951. https://doi.org/10.1016/j.jhydrol.2019.03.077

Di Prima, S., Concialdi, P., Lassabatere, L., Angulo-Jaramillo, R., Pirastru, M., Cerda, A., Keesstra, S., 2018a. Laboratory testing of Beerkan infiltration experiments for assessing the role of soil sealing on water infiltration. CATENA 167, 373–384. https://doi.org/10.1016/j.catena.2018.05.013

Di Prima, S., Lassabatere, L., Bagarello, V., Iovino, M., Angulo-Jaramillo, R., 2016. Testing a new automated single ring infiltrometer for Beerkan infiltration experiments. Geoderma 262, 20–34. https://doi.org/10.1016/j.geoderma.2015.08.006

Di Prima, S., Lassabatere, L., Rodrigo-Comino, J., Marrosu, R., Pulido, M., Angulo-Jaramillo, R., Úbeda, X., Keesstra, S., Cerdà, A., Pirastru, M., 2018b. Comparing Transient and Steady-State Analysis of Single-Ring Infiltrometer Data for an Abandoned Field Affected by Fire in Eastern Spain. Water 10. https://doi.org/10.3390/w10040514

Di Prima, S., Marrosu, R., Lassabatere, L., Angulo-Jaramillo, R., Pirastru, M., 2018c. In situ characterization of preferential flow by combining plot- and point-scale infiltration experiments on a hillslope. Journal of Hydrology 563, 633–642. https://doi.org/10.1016/j.jhydrol.2018.06.033

Durand, C., Ruban, V., Amblès, A., 2005. Characterisation of complex organic matter present in contaminated sediments from water retention ponds. Journal of Analytical and Applied Pyrolysis 73, 17–28. https://doi.org/10.1016/j.jaap.2004.09.001

Elrick, D.E., Reynolds, W.D., 1992. Methods for analyzing constant-head well permeameter data. Soil Science Society of America Journal 56, 320. https://doi.org/10.2136/sssaj1992.03615995005600010052x

Gardner, W., 1958. Some steady-state solutions of the unsaturated moisture flow equation with application to evaporation from a water table. Soil science 85, 228–232.

Goebel, M.-O., Bachmann, J., Reichstein, M., Janssens, I.A., Guggenberger, G., 2011. Soil water repellency and its implications for organic matter decomposition – is there a link to extreme climatic events? Global Change Biology 17, 2640–2656. https://doi.org/10.1111/j.1365-2486.2011.02414.x

Haverkamp, R., Bouraoui, F., Zammit, C., Angulo-Jaramillo, R., 1999. Soil properties and moisture movement in the unsaturated zone. Handbook of groundwater engineering.

Haverkamp, R., Parlange, J.-Y., Starr, J., Schmitz, G., Fuentes, C., 1990. Infiltration under ponded conditions: 3. A predictive equation based on physical parameters. Soil science 149, 292–300. https://doi.org/10.1097/00010694-199005000-00006

Haverkamp, R., Ross, P.J., Smettem, K.R.J., Parlange, J.Y., 1994. Three-dimensional analysis of infiltration from the disc infiltrometer: 2. Physically based infiltration equation. Water Resour. Res. 30, 2931–2935. https://doi.org/10.1029/94WR01788

Hinnell, A.C., Lazarovitch, N., Warrick, A.W., 2009. Explicit infiltration function for boreholes under constant head conditions: INFILTRATION FUNCTION FOR BOREHOLES. Water Resources Research 45, n/a-n/a. https://doi.org/10.1029/2008WR007685

Khaleel, R., Relyea, J.F., 2001. Variability of Gardner's α for coarse-textured sediments. Water Resources Research 37, 1567–1575. https://doi.org/10.1029/2000WR900398

Lassabatere, L., Angulo-Jaramillo, R., Soria Ugalde, J.M., Cuenca, R., Braud, I., Haverkamp, R., 2006. Beerkan estimation of soil transfer parameters through infiltration experiments—BEST. Soil Science Society of America Journal 70, 521. https://doi.org/10.2136/sssaj2005.0026

Mertens, J., Jacques, D., Vanderborght, J., Feyen, J., 2002. Characterisation of the field-saturated hydraulic conductivity on a hillslope: in situ single ring pressure infiltrometer measurements. Journal of Hydrology 263, 217–229. https://doi.org/10.1016/S0022-1694(02)00052-5

Mualem, Y., 1976. A new model for predicting the hydraulic conductivity of unsaturated porous media. Water Resour. Res 12, 513–522.

Nimmo, J.R., Schmidt, K.M., Perkins, K.S., Stock, J.D., 2009. Rapid Measurement of Field-Saturated Hydraulic Conductivity for Areal Characterization. Vadose Zone Journal 8, 142. https://doi.org/10.2136/vzj2007.0159

Parlange, J.-Y., 1975. Convergence and validity of time expansion solutions: a comparison to exact and approximate solutions. Soil Science Society of America Journal 39, 3–6.

Philip, J., 1957. The theory of infiltration: 4. Sorptivity and algebraic infiltration equations. Soil sci 84, 257–264.

Philip, J.R., 1985. Reply To "Comments on Steady Infiltration from Spherical Cavities." Soil Science Society of America Journal 49, 788–789. https://doi.org/10.2136/sssaj1985.03615995004900030055x

Philip, J.R., 1968. Steady Infiltration From Buried Point Sources and Spherical Cavities. Water Resources Research 4, 1039–1047. https://doi.org/10.1029/WR004i005p01039

Raats, P.A.C., 1976. Analytical Solutions of a Simplified Flow Equation. Transactions of the ASAE 19, 0683–0689. https://doi.org/10.13031/2013.36096

Reynolds, W., Elrick, D., 2002. 3.4.3.2.b Pressure infiltrometer. In Methods of Soil Analysis, Part 4, PhysicalMethods, Dane JH, Topp GC (eds). SSSA Book Series, No. 5. Soil Sci. Soc. Am.: Madison,Wisconsin, USA 4, 826–836.

Reynolds, W., Elrick, D., Youngs, E., 2002. 3.4.3.2 Ring or cylinder infiltrometers (vadose zone). In Methods of Soil Analysis, Part 4, PhysicalMethods, Dane JH, Topp GC (eds). SSSA Book Series, No. 5. Soil Sci. Soc. Am.: Madison,Wisconsin, USA 818–820.

Reynolds, W.D., 2013. An assessment of borehole infiltration analyses for measuring field-saturated hydraulic conductivity in the vadose zone. Engineering Geology 159, 119–130. https://doi.org/10.1016/j.enggeo.2013.02.006

Reynolds, W.D., 1994. Letter to the editor. Comment on "comparison of three methods for assessing soil hydraulic properties" by G. B. Paige and D. Hillel. Soil Science 157, 120.

Reynolds, W.D., Elrick, D.E., 2002. 3.4.3.3 Constant Head Well Permeameter (Vadose Zone), in: Methods of Soil Analysis: Part 4 Physical Methods, SSSA Book Series. Soil Science Society of America, Madison, WI, pp. 844–858. https://doi.org/10.2136/sssabookser5.4.c33

Reynolds, W.D., Elrick, D.E., 1990. Ponded Infiltration From a Single Ring: I. Analysis of Steady Flow. Soil Science Society of America Journal 54, 1233. https://doi.org/10.2136/sssaj1990.03615995005400050006x

Rillig, M.C., Mardatin, N.F., Leifheit, E.F., Antunes, P.M., 2010. Mycelium of arbuscular mycorrhizal fungi increases soil water repellency and is sufficient to maintain water-stable soil aggregates. Soil Biology and Biochemistry 42, 1189–1191. https://doi.org/10.1016/j.soilbio.2010.03.027
Russo, D., Russo, I., Laufer, A., 1997. On the spatial variability of parameters of the unsaturated hydraulic conductivity. Water Resources Research 33, 947–956. https://doi.org/10.1029/96WR03947
Smettem, K.R.J., Parlange, J.Y., Ross, P.J., Haverkamp, R., 1994. Three-dimensional analysis of infiltration from the disc infiltrometer: 1. A capillary-based theory. Water Resour. Res. 30, 2925–2929. https://doi.org/10.1029/94WR01787
Smith, R.E., Smettem, K.R., Broadbridge, P., 2002. Infiltration theory for hydrologic applications. American Geophysical Union.
Stewart, R.D., Abou Najm, M.R., 2018a. A Comprehensive Model for Single Ring Infiltration I: Initial Water Content and Soil Hydraulic Properties. Soil Science Society of America Journal 82, 548–557. https://doi.org/10.2136/sssaj2017.09.0313
Stewart, R.D., Abou Najm, M.R., 2018b. A Comprehensive Model for Single Ring Infiltration II: Estimating Field-Saturated Hydraulic Conductivity. Soil Science Society of America Journal 82, 558–567. https://doi.org/10.2136/sssaj2017.09.0314
van Genuchten, M.T., 1980. A closed-form equation for predicting the hydraulic conductivity of unsaturated soils. Soil science society of America journal 44, 892–898.
White, I., Sully, M.J., 1992. On the variability and use of the hydraulic conductivity alpha parameter in stochastic treatments of unsaturated flow. Water Resour. Res. 28, 209–213. https://doi.org/10.1029/91WR02198
White, I., Sully, M.J., 1987. Macroscopic and microscopic capillary length and time scales from field infiltration. Water Resour. Res. 23, 1514–1522. https://doi.org/10.1029/WR023i008p01514
Wooding, R.A., 1968. Steady Infiltration from a Shallow Circular Pond. Water Resour. Res. 4, 1259–1273. https://doi.org/10.1029/WR004i006p01259
Wu, L., Pan, L., Mitchell, J., Sanden, B., 1999. Measuring Saturated Hydraulic Conductivity using a Generalized Solution for Single-Ring Infiltrometers. Soil Science Society of America Journal 63, 788. https://doi.org/10.2136/sssaj1999.634788x
Xu, X., Lewis, C., Liu, W., Albertson, J.D., Kiely, G., 2012. Analysis of single-ring infiltrometer data for soil hydraulic properties estimation: Comparison of BEST and Wu methods. Agricultural Water Management 107, 34–41. https://doi.org/10.1016/j.agwat.2012.01.004

Table E. Relationships for calculating the saturated soil hydraulic conductivity, K_s, by the One-Ponding Depth (OPD) method, the method 2 by Wu et al. (1999) (WU2), the Steady version of the Simplified method based on a Beerkan Infiltration run (SSBI), and the Approach 4 (A4).

Relationships			
OPD	WU2	SSBI	A4
$K_s = \frac{\frac{i_s \pi r^2}{\lambda_c}\left(0.316\frac{d}{r}+0.184\right)}{r\left(\frac{H}{\lambda_c}+1\right)+\left(0.316\frac{d}{r}+0.184\right)\frac{\pi r^2}{\lambda_c}}$ (t1)	$K_s = \frac{i_s}{0.9084\left(\frac{H+\lambda_c}{G^*}+1\right)}$ (t2)	$K_s = \frac{i_s}{\frac{\gamma \gamma_w \lambda_c}{r}+1}$ (t3)	$K_s = \frac{i_s}{\left(\frac{H+\lambda_c}{G^*}+1\right)}$ (t4)

Parameters
d (L) = ring insertion depth into the soil.
$G^* = d + r/2$.
H (L) = ponding depth of water.
i_s (L T^{-1}) = steady-state infiltration rate estimated from the cumulative infiltration versus time plot.
λ_c (L) = macroscopic capillary length.
r (L) = ring radius.
γ = dimensionless constant set equal to 0.75 and related to the effect of disk curvature and gravity (Smettem et al., 1994).
γ_w = dimensionless constant related to the shape of the wetting front (White and Sully, 1987). A value of γ_w = 1.818 was suggested by Reynolds and Elrick (2002).

Table C. Soil hydraulic parameters for the five studied soils used to model the infiltration experiments. From Carsel and Parrish (1988).

Soil texture	Sand	Loamy Sand	Sandy Loam	Loam	Silt Loam	Silty Clay Loam
θ_r	0.045	0.057	0.065	0.078	0.067	0.089
θ_s	0.43	0.41	0.41	0.43	0.45	0.43
α_{VG} (mm^{-1})	0.0145	0.0124	0.0075	0.0036	0.002	0.001
n	2.68	2.28	1.89	1.56	1.41	1.23
$\widehat{K}_s$ ($mm\ h^{-1}$)	297.0	145.9	44.2	10.44	4.5	0.7
l	0.5	0.5	0.5	0.5	0.5	0.5

Table L. Soil capillarity categories suggested by Elrick and Reynolds (1992), and representative α (mm^{-1}) and λ_c (mm) values. The suggested range values for the two parameters are also reported.

Soil capillarity category	Representative α (mm^{-1})	Suggested α range values	Representative λ_c (mm)	λ_c range values
Very strong	≤ 0.001		≥ 1000	
Strong	0.004	$0.001<\alpha<0.008$	250	$125<\lambda_c<1000$
Moderate	0.012	$0.008\leq\alpha\leq 0.024$	83	$42\leq\lambda_c\leq 125$
Weak	0.036	$0.024<\alpha<0.1$	28	$10<\lambda_c<42$
Negligible	≥ 0.1		≤ 10	

Table S. Summary of the Beerkan infiltration database. Total number of Beerkan infiltration experiments, N_{tot} = 433.

Country	Site	*N*	*D* (cm)	*V* (mL)	Coordinates	Reference
Burundi	Nyamutobo (Ruyigi)	77	15	150	3°27'50" S, 30°15'40" E	Bagarello et al. (2011)
Burundi	Kinyami (Ngozi)	20	15	150	2°54'30" S, 29°49'06" E	
Italy	Giampilieri	11	15	150	38°4'8" N, 15°28'26" E	Bagarello et al. (2013)
Italy	Palermo - SAAF† (Sicily)	8	30	800	38°6'25" N, 13°21'6" E	Bagarello et al. (2014b)
Italy	Caccamo (Sicily)	4	30	800	37°52'34" N, 13°38'43" E	
Italy	Corleone (Sicily)	20	30	800	37°48'35" N, 13°17'49" E	
Italy	Sparacia (Sicily)	8	30	800	37°38'11" N, 13°45'50" E	
Italy	Palermo - SAAF (Sicily)	10	8.5	64	38°6'25" N, 13°21'6" E	Bagarello et al. (2014a)
Italy	Sparacia (Sicily)	10	8.5	64	37°38'10" N, 13°45'59" E	
Italy	Palermo - Parco d'Orleans (Sicily)	10	8.5	64	38°6'26" N, 13°20'59" E	
Italy	Villabate (Sicily)	10	8.5	64	38°4'53" N, 13°25'7" E	
Italy	Palermo - SAAF (Sicily)	12	15	200	38°6'25" N, 13°21'6" E	Bagarello et al. (2014c)
Italy	Palermo - SAAF (Sicily)	4	30	800	38°6'25" N, 13°21'6" E	
Italy	Pietranera (Sicily)	4	15	200	37°32'25" N, 13°30'44" E	
Italy	Pietranera (Sicily)	4	30	800	37°32'25" N, 13°30'44" E	
Italy	Caccamo (Sicily)	4	15	200	37°52'34" N, 13°38'43" E	
Italy	Corleone (Sicily)	20	15	200	37°48'35" N, 13°17'49" E	
Italy	Sparacia (Sicily)	8	15	200	37°38'11" N, 13°45'50" E	
Burundi	Nyamutobo (Ruyigi)	75	15	150	3°27'50" S, 30°15'40" E	
Italy	Palermo - Parco d'Orleans (Sicily)	10	15	150	38°6'26" N, 13°20'59" E	Alagna et al. (2016b)
Italy	Palermo - SAAF (Sicily)	10	15	150	38°6'25" N, 13°21'6" E	Di Prima et al. (2016)
Italy	Palermo - Parco d'Orleans (Sicily)	10	15	150	38°6'26" N, 13°20'59" E	
Italy	Sparacia (Sicily)	10	15	150	37°38'10" N, 13°45'59" E	
France	Crépieux-Charmy (Lyon)	9	15	150	45°47'42" N, 4°53'19" E	
Spain	Les Alcusses de Moixent (Valencia)	10	8.5	48	38°48'33"N, 0°49'3"O	Di Prima et al. (2017)
Italy	Palermo - SAAF (Sicily)	5	5	17	38°6'25" N, 13°21'6" E	Di Prima et al. (2018a)
Italy	Palermo - Parco d'Orleans (Sicily)	5	5	17	38°6'26" N, 13°20'59" E	
Italy	Sparacia (Sicily)	5	5	17	37°38'10" N, 13°45'59" E	
Italy	Baratz Lake watershed (Sardinia)	40	8	43	40°41'53" N, 8°14'4" E	Di Prima et al. (2018c)

† Department of Agricultural, Food and Forest Sciences (SAAF = Scienze Agrarie, Alimentari e Forestali).
N = Number of Beerkan infiltration experiments; *D* (cm) = ring diameter; *V* (mL) = water volume applied with each pouring.

Table P. Summary of the soil hydraulic properties for the six synthetic soils.

Soil	Se	h_i (mm)	θ_i (m^3m^{-3})	S ($mm\ h^{-0.5}$) (Eq. 12)	ϕ ($mm^2\ h^{-1}$) (Eq. 3)	$\hat{\lambda}_c$ (mm) (Eq. 2)	λ_c (mm) (Eq. 8)	i_s ($mm\ h^{-1}$)	b_s (mm)	K_s ($mm\ h^{-1}$)			
										OPD (Eq. t1)	WU2 (Eq. t2)	SSBI (Eq. t3)	A4 (Eq. t4)
Sand	0.1	269.0	0.083	86.5	11308.6	38.1	37.2	516.7	15.0	304.3	319.1	341.3	289.8
	0.2	174.5	0.122	81.3	11298.6	38.0	37.0	515.3	13.2	304.2	319.0	341.0	289.7
	0.3	133.1	0.160	75.7	11268.5	37.9	36.8	513.3	11.5	303.7	318.5	340.3	289.3
	0.4	107.8	0.199	69.6	11202.4	37.7	36.7	510.6	9.8	302.4	317.2	338.8	288.1
	0.5	89.7	0.237	62.9	11076.7	37.3	36.7	506.5	8.2	299.8	314.4	335.9	285.6
	0.6	75.2	0.276	55.5	10854.0	36.5	37.1	500.4	6.6	294.9	309.2	330.7	280.9
	0.7	62.5	0.314	46.9	10467.3	35.2	38.2	491.1	5.1	286.1	299.8	321.6	272.3
	0.8	50.2	0.353	36.8	9776.1	32.9	40.5	476.0	3.6	270.3	282.7	305.4	256.8
Loamy Sand	0.1	483.8	0.092	58.2	5602.2	38.4	37.4	254.5	13.8	149.5	156.7	167.8	142.4
	0.2	276.4	0.128	54.7	5598.0	38.4	37.2	253.8	12.2	149.5	156.7	167.6	142.4
	0.3	195.6	0.163	50.9	5584.2	38.3	36.9	252.8	10.6	149.3	156.6	167.4	142.3
	0.4	150.0	0.198	46.8	5552.5	38.1	36.6	251.4	9.0	149.0	156.2	166.9	141.9
	0.5	119.2	0.233	42.3	5490.2	37.6	36.4	249.3	7.5	148.1	155.4	165.8	141.2
	0.6	95.9	0.269	37.3	5376.9	36.9	36.3	246.1	6.0	146.4	153.6	163.9	139.5
	0.7	76.5	0.304	31.5	5176.0	35.5	36.5	241.3	4.5	143.2	150.2	160.4	136.5
	0.8	58.9	0.339	24.6	4811.2	33.0	37.4	233.4	3.1	137.2	143.8	153.9	130.6
Sandy Loam	0.1	1765.2	0.100	36.0	2145.5	49.7	48.3	86.5	17.4	45.4	47.2	52.1	42.9
	0.2	799.2	0.134	33.8	2145.5	49.7	48.0	86.3	15.4	45.4	47.2	52.0	42.9
	0.3	494.2	0.169	31.5	2140.3	49.5	47.6	85.9	13.4	45.4	47.2	52.0	42.9
	0.4	344.1	0.203	29.0	2129.8	49.3	47.1	85.3	11.3	45.3	47.2	51.8	42.9
	0.5	253.1	0.238	26.2	2107.9	48.8	46.5	84.5	9.3	45.2	47.0	51.6	42.7
	0.6	190.3	0.272	23.1	2066.0	47.8	45.7	83.3	7.3	44.8	46.7	51.2	42.5
	0.7	142.4	0.307	19.5	1988.8	46.0	44.9	81.4	5.4	44.2	46.1	50.3	41.8
	0.8	102.3	0.341	15.2	1843.8	42.7	44.0	78.1	3.5	42.8	44.6	48.7	40.6
Loam	0.1	16941.8	0.113	20.9	719.7	69.2	67.6	24.3	24.9	10.7	11.0	12.6	10.0
	0.2	4883.1	0.148	19.6	719.6	69.2	67.2	24.2	22.0	10.7	11.0	12.6	10.0
	0.3	2330.8	0.184	18.3	718.8	69.1	66.6	24.1	19.1	10.7	11.0	12.6	10.0
	0.4	1354.4	0.219	16.8	716.5	68.9	65.9	23.9	16.2	10.7	11.0	12.6	10.0
	0.5	866.2	0.254	15.2	711.0	68.4	64.8	23.7	13.2	10.7	11.0	12.6	10.0
	0.6	579.6	0.289	13.4	699.3	67.2	63.2	23.3	10.3	10.7	11.0	12.5	10.0
	0.7	390.5	0.324	11.3	676.0	65.0	61.0	22.7	7.5	10.6	10.9	12.4	9.9
	0.8	252.5	0.360	8.8	629.2	60.5	57.7	21.6	4.7	10.4	10.8	12.1	9.8
Silt Loam	0.1	1.4×10^5	0.105	16.3	402.8	89.5	87.8	12.3	35.1	4.6	4.7	5.6	4.3
	0.2	25267.3	0.144	15.3	402.8	89.5	87.3	12.2	31.1	4.6	4.7	5.6	4.3
	0.3	9318.5	0.182	14.3	402.6	89.5	86.6	12.2	27.0	4.6	4.7	5.6	4.3
	0.4	4529.8	0.220	13.2	401.8	89.3	85.7	12.1	22.9	4.6	4.7	5.6	4.3
	0.5	2531.6	0.258	11.9	399.6	88.8	84.4	12.0	18.8	4.6	4.7	5.6	4.3
	0.6	1519.5	0.297	10.5	394.4	87.6	82.4	11.8	14.7	4.6	4.7	5.6	4.3
	0.7	933.0	0.335	8.9	383.2	85.2	79.3	11.5	10.6	4.6	4.7	5.5	4.3
	0.8	553.5	0.373	7.0	359.1	79.8	74.2	10.9	6.6	4.6	4.7	5.4	4.3
Silty Clay Loam	0.1	2.2×10^7	0.123	6.0	60.0	85.7	84.9	1.9	30.3	0.7	0.7	0.9	0.7
	0.2	1.1×10^6	0.157	5.6	60.0	85.7	84.5	1.9	26.8	0.7	0.7	0.9	0.7
	0.3	$1.9E\times10^5$	0.191	5.2	60.0	85.7	84.1	1.9	23.3	0.7	0.7	0.9	0.7
	0.4	53399.3	0.225	4.8	60.0	85.7	83.4	1.9	19.8	0.7	0.7	0.9	0.7
	0.5	19954.8	0.259	4.4	59.9	85.5	82.5	1.8	16.3	0.7	0.7	0.9	0.7
	0.6	8725.5	0.294	3.9	59.5	85.0	81.0	1.8	12.8	0.7	0.7	0.9	0.7
	0.7	4137.5	0.328	3.3	58.5	83.6	78.5	1.8	9.3	0.7	0.7	0.9	0.7
	0.8	1966.9	0.362	2.6	55.9	79.9	73.6	1.7	5.8	0.7	0.7	0.9	0.7

Table Q. Summary of the soil hydraulic properties estimated from the Beerkan database.

Statistic	λ_c (mm) (Eq. 8)	K_s (mm h^{-1})				
		BEST-steady (Eq. 15)	OPD (Eq. t1)	WU2 (Eq. t2)	SSBI (Eq. t3)	A4 (Eq. t4)
N	427	427	427	427	427	427
min	1.5	1.3	1.4	1.4	1.6	1.2
max	737.7	3550.9	3294.1	3493.8	3758.7	3173.7
mean	112.6	270.7	258.5	269.3	305.2	244.6
median	68.0	156.8	153.3	156.4	182.4	142.0
CV	101.3	142.0	140.1	141.3	137.6	141.3

Figure H. Cumulative infiltration curves for different soils and initial effective saturation degrees, *Se*. The curve were generated analytically using Eqs. (10) and (11) and the parameters listed in **Table C**. The labels in ordinate and abscissa report respectively the total infiltrated water and the duration of the infiltration process. Note that the duration was fixed at three times the maximum time ($3 \times t_{max}$).

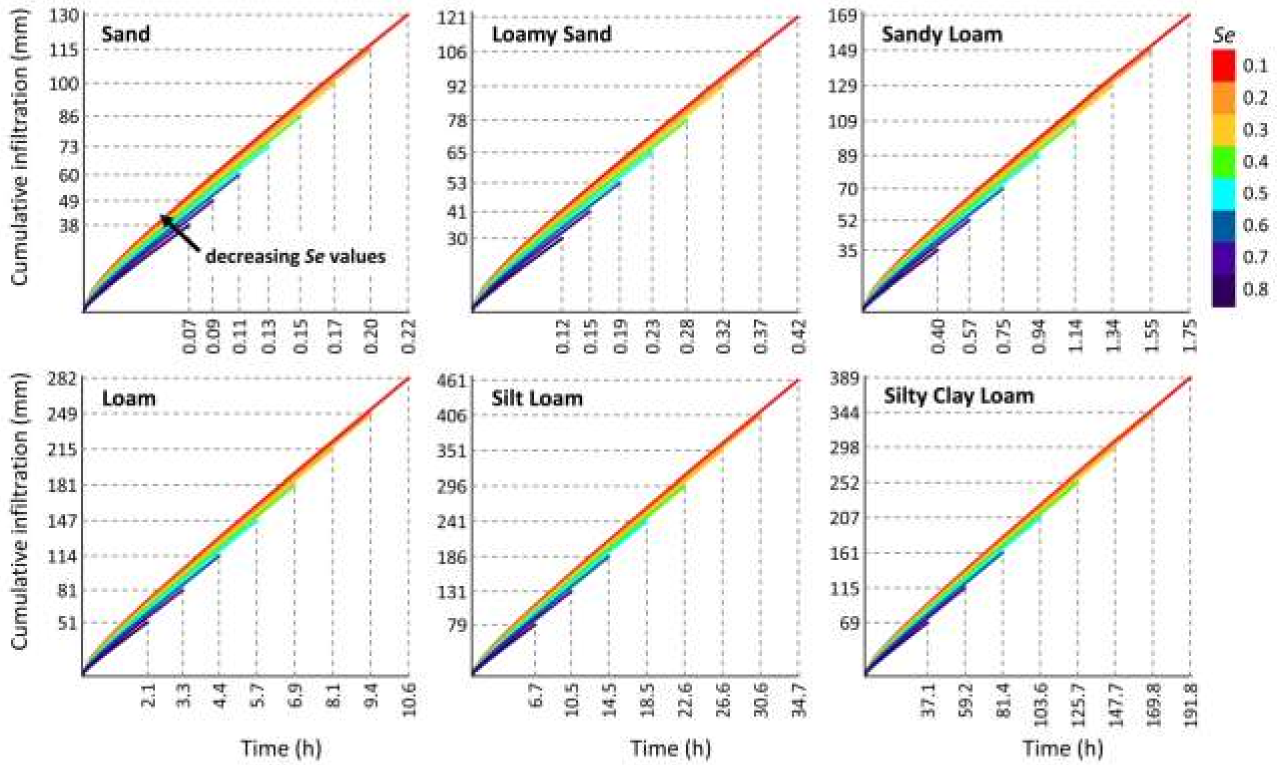

Figure G. Values of the relative error of the macroscopic capillary length, $Er(\lambda_c)$, predictions (expressed as a percentage of the actual values, $\hat{\boldsymbol{\lambda}}_{\boldsymbol{c}}$) estimated for the six synthetic soils listed in **Table C**.

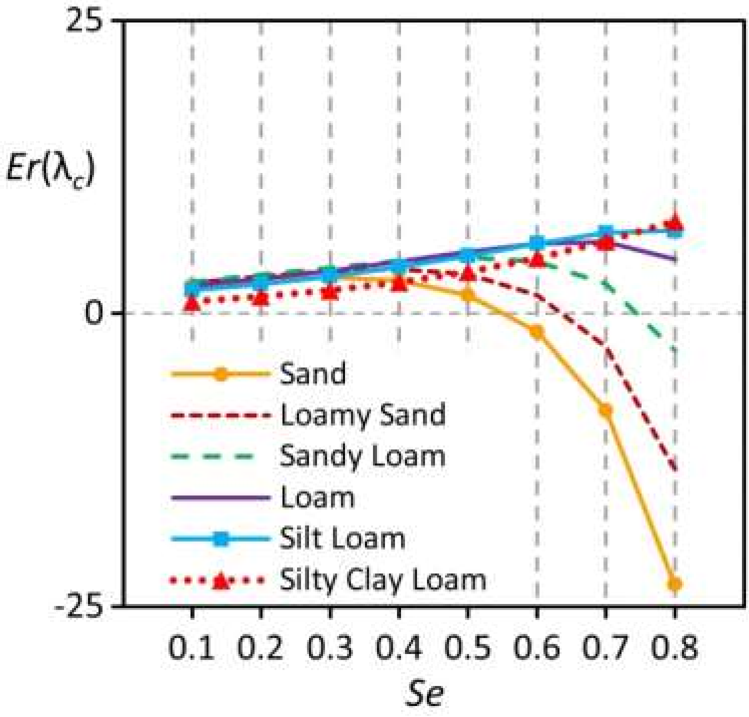

Figure K. Hydraulic conductivity functions of the six synthetic soils listed in **Table C**.

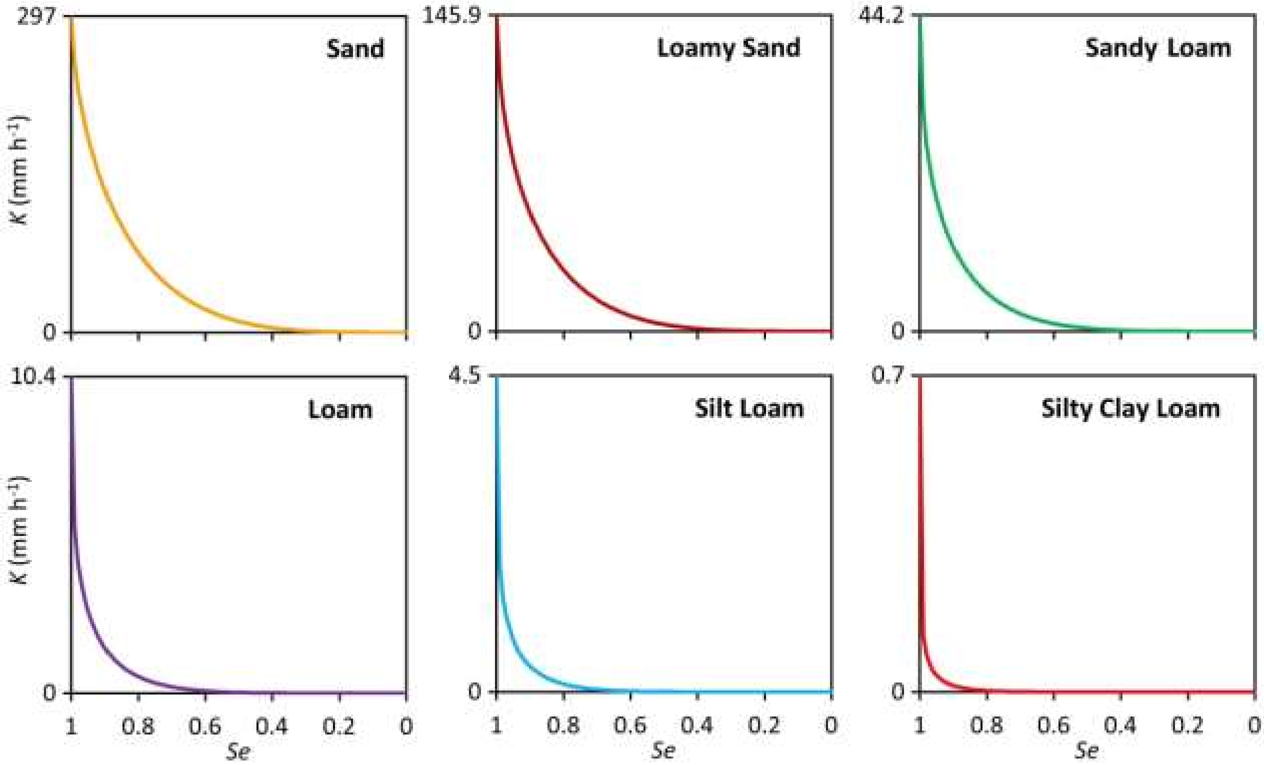

Figure W. Values of the relative error of the saturated soil hydraulic conductivity, $Er(K_s)$, predictions (expressed as a percentage of the actual values, $\widehat{\boldsymbol{K}}_{\boldsymbol{s}}$) estimated for the six synthetic soils by the four considered methods (i.e., OPD, WU2, SSBI, A4).

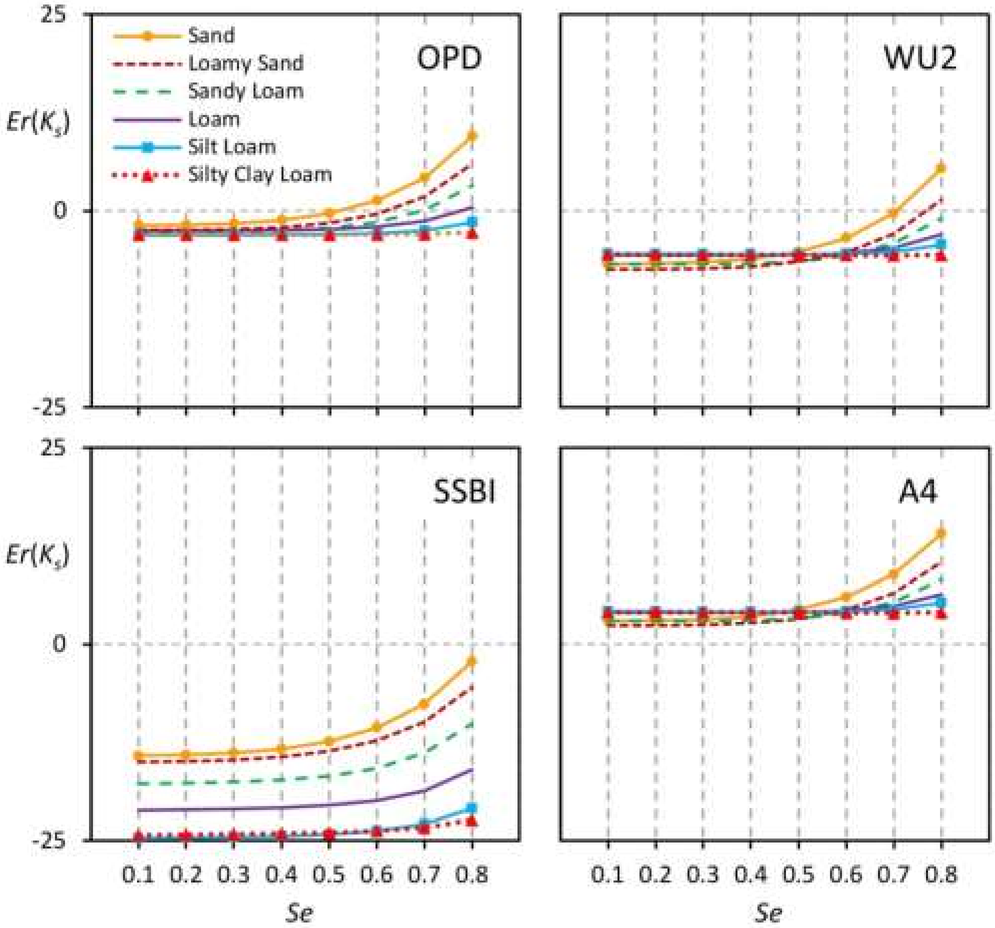

Figure T. Textural triangle and textural properties of the soils included in the Beerkan infiltration database.

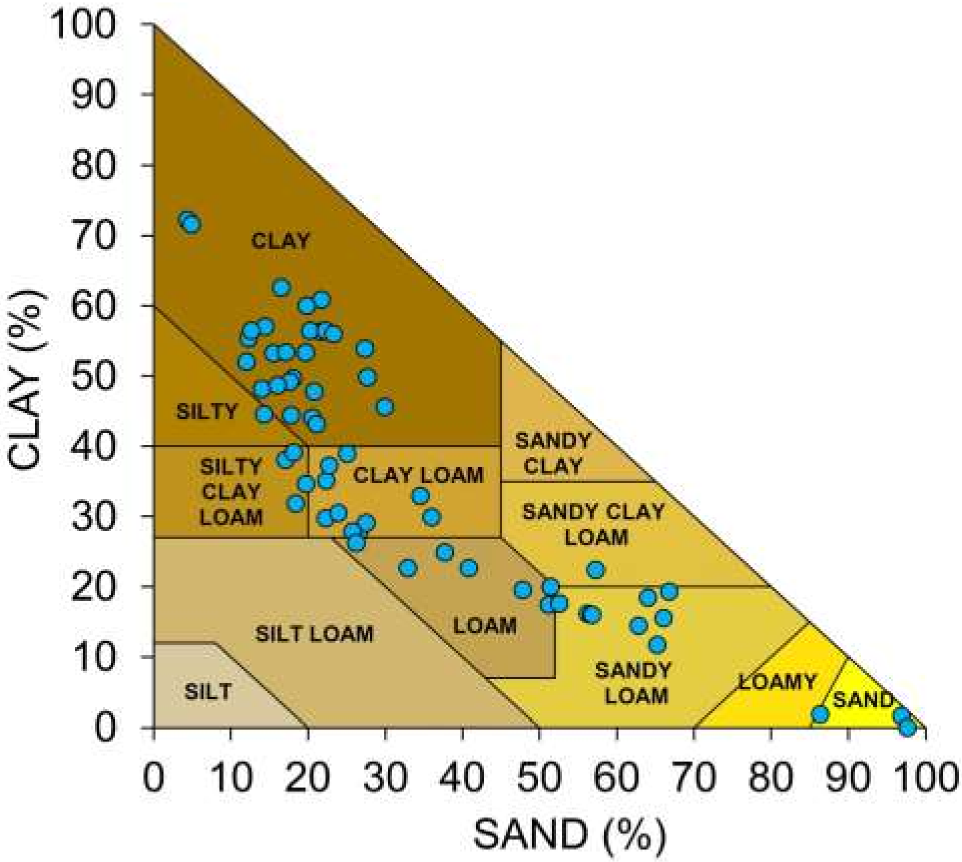

Figure F. **(a)** Comparison between the estimated macroscopic capillary length, λ_c, and the intercept, b_s, values. The soil capillarity categories are also reported. **(a) (b) (c)** Examples of estimation of λ_c in case of **(b)** moderate, **(c)** strong, and **(d)** negligible capillarity conditions.

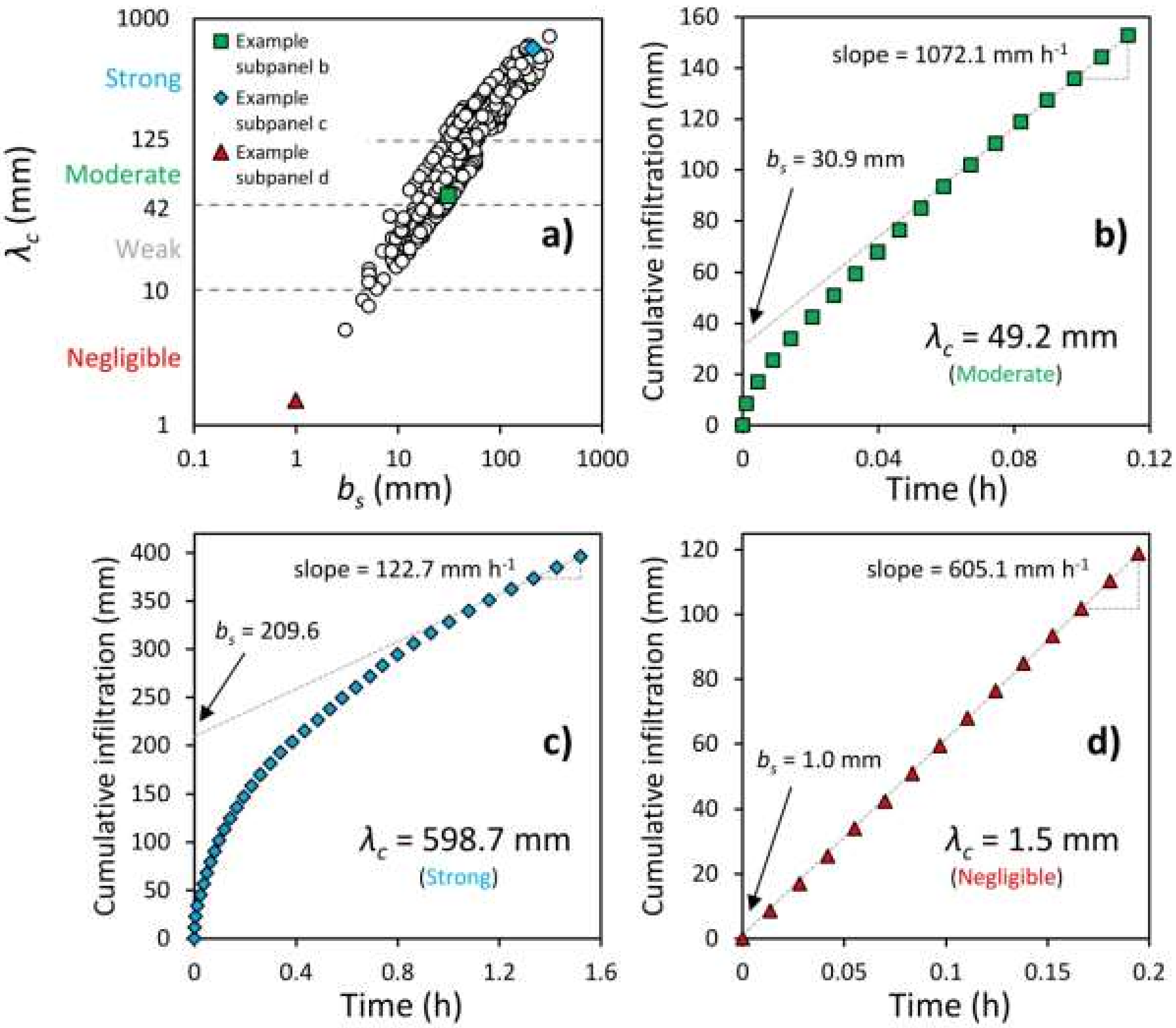

Figure D. Sample size, N, of the macroscopic capillary length predictions and mean sand content (%) for each soil capillarity category.

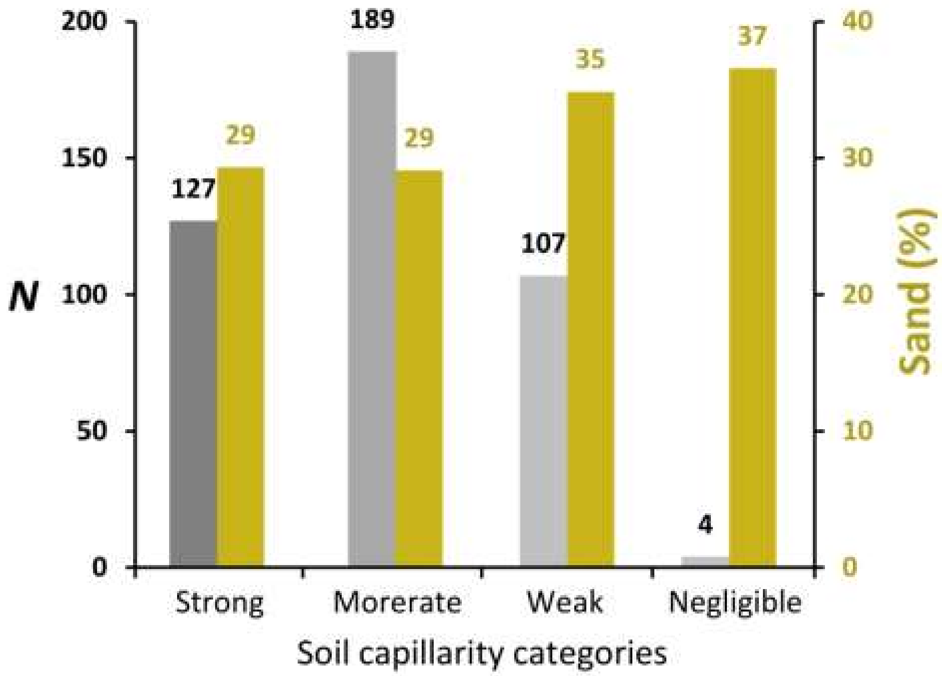

Figure Z. Cumulative empirical frequency distribution of the saturated soil hydraulic conductivity, $Er(K_s)$, predictions (expressed as a percentage of the BEST-deduced values, $K_{s,BEST}$), estimated for the six considered soils by the four considered methods (i.e., OPD, WU2, SSBI, A4).